

Photocatalytic Activities and Crystal Structures of Titanium Dioxide by Anodization: Their Dependence upon Current Density

Yoshiteru Mizukoshi and Naoya Masahashi

Osaka Center for Industrial Materials Research, Institute for Materials Research, Tohoku University, Sakai 599-8531, Japan

The crystal structure, crystallinity and surface area of anodized TiO₂ were systematically investigated focusing on the current density in the anodization. Anatase phase was evolved with an increase of the current density for the anodic oxides prepared in the electrolyte of 0.1 mol·L⁻¹ sulfuric acid, and the surface area was almost constant against the current density. On the other hand, rutile phase was evolved with the same of 1.2 mol·L⁻¹ sulfuric acid, and the surface area increased with the current density. Photocatalytic degradation rates of methylene blue (MB) were normalized by surface area of TiO₂, showing that the maximum value was found in the anodic oxide with approximately 60% of rutile in the fraction. The specific rate constant for MB degradation was the best in the anodic oxide with low lattice strain and the crystallite size of appropriately 40 nm. [doi:10.2320/matertrans.M2010106]

(Received March 24, 2010; Accepted June 3, 2010; Published July 14, 2010)

Keywords: anodization, crystallinity, titanium, photocatalyst, current density

1. Introduction

TiO₂ is regarded as one of the most promising photocatalysts due to its broad functionality, long-term stability and non-toxicity since the first discovery by Honda and Fujishima.¹⁾ A number of methods have been employed to fabricate the TiO₂ such as sol-gel methods,²⁾ thermal chemical vapor deposition,³⁾ thermal spraying,⁴⁾ and sputtering,⁵⁾ along with anodic⁶⁻⁹⁾ and thermal oxidation.¹⁰⁾ Recently, we have reported the fabrication of TiO₂ photocatalyst on Ti or Ti alloy substrate by anodic oxidation. So far, it was reported that TiO₂ anodized in a sulfuric acid aqueous solution effectively degraded methylene blue (MB) aqueous solution¹¹⁾ and exhibited superhydrophilicity.¹²⁾ In addition, the anodic oxide showed photocatalytic activity under visible light illumination probably due to the band gap narrowing by sulfur doping.¹³⁾ In the anodic oxidation, various parameters such as concentration of electrolytes, applied voltage, pH and temperature, affect the characteristics of the produced oxide film. Among the parameters, especially from the industrial view point, current density is important because it determines the sizes of the anode substrates and specifications of the DC power supply. However, relevant reports on the effect of current density of anodization upon the photocatalytic activity are quite few.¹⁴⁾

In the present study, we examined the effect of current density during anodic oxidation on the photocatalytic activities focusing on the microstructure and crystal structure of the oxide. The current density was systematically varied and the obtained TiO₂ was characterized by XRD, SEM, and laser microscope. The characteristic of the anodized TiO₂ determining the photocatalytic activities were explored.

2. Experimental

A pure Ti plate (cp-Ti, grade I) with dimensions of 19 × 9 × 1 mm³ that was to be used as the anode was chemically polished using a 40-nm colloidal silica suspension and was thoroughly washed in ethanol using an

ultrasonic cleaner. A constant current of 8–400 mA corresponding to current density of 20–1000 A·m⁻² was applied to the Ti plate for 0.5 h in a sulfuric acid electrolyte of 0.1 or 1.2 mol·L⁻¹. A Pt mesh electrode (5 × 5 cm²) was used as the cathode. The anodized Ti was rinsed with distilled water and then dried at room temperature, followed by annealing at 723 K for 5 h in air atmosphere. We previously reported that the thickness of the oxide did not change with annealing, but the crystallinity of the oxide was improved to provide better photocatalytic activity for MB bleaching.¹¹⁾ The crystallographic structure of the anodized oxide was determined by X-ray diffraction (PANalytical X'Pert diffractometer, Netherlands) with CuK_α radiation (0.15406 nm), at a scan rate of 1° min⁻¹, and a rotating detector. The sample was set in a thin-film geometry arrangement at 0.5° glancing angle. Microstructure observations were conducted with a scanning electron microscopy (Keyence VE-8800, Japan) at an operating voltage of 20 kV. Surface area was measured using a laser microscope with a wavelength of 408 nm (Keyence VK-9710, Japan).

The photocatalytic activities of the fabricated photocatalysts were evaluated by degradation of MB in aqueous solutions. The evaluations were carefully done considering the adsorption of MB molecules on the surface of the TiO₂, the direct photolysis of MB molecules and the self-sensitizing degradation due to MB absorption. Prior to the evaluations, the TiO₂ were immersed in 0.02 mol·L⁻¹ MB aqueous solution for more than 12 h, and the saturation of MB adsorptions were confirmed. After the pre-treatment, the degradation of MB was carried out using 0.01 mol·L⁻¹ MB solution. Light illumination was conducted by UV lamp with the central wavelength at 365 nm and full width at half maximum of 36 nm through bandpass filter. The passed light intensity through the 10 mm thickness of 0.01 mol·L⁻¹ MB solution at the surface of the photocatalysts was regulated at 5 W m⁻². The concentration of MB was determined from the absorbance at 664 nm measured with a UV-vis spectrophotometer (Jasco V-550, Japan). Several experimental results indicated that the photocatalytic decomposition of various dyes over illuminated TiO₂ fitted the Langmuir–

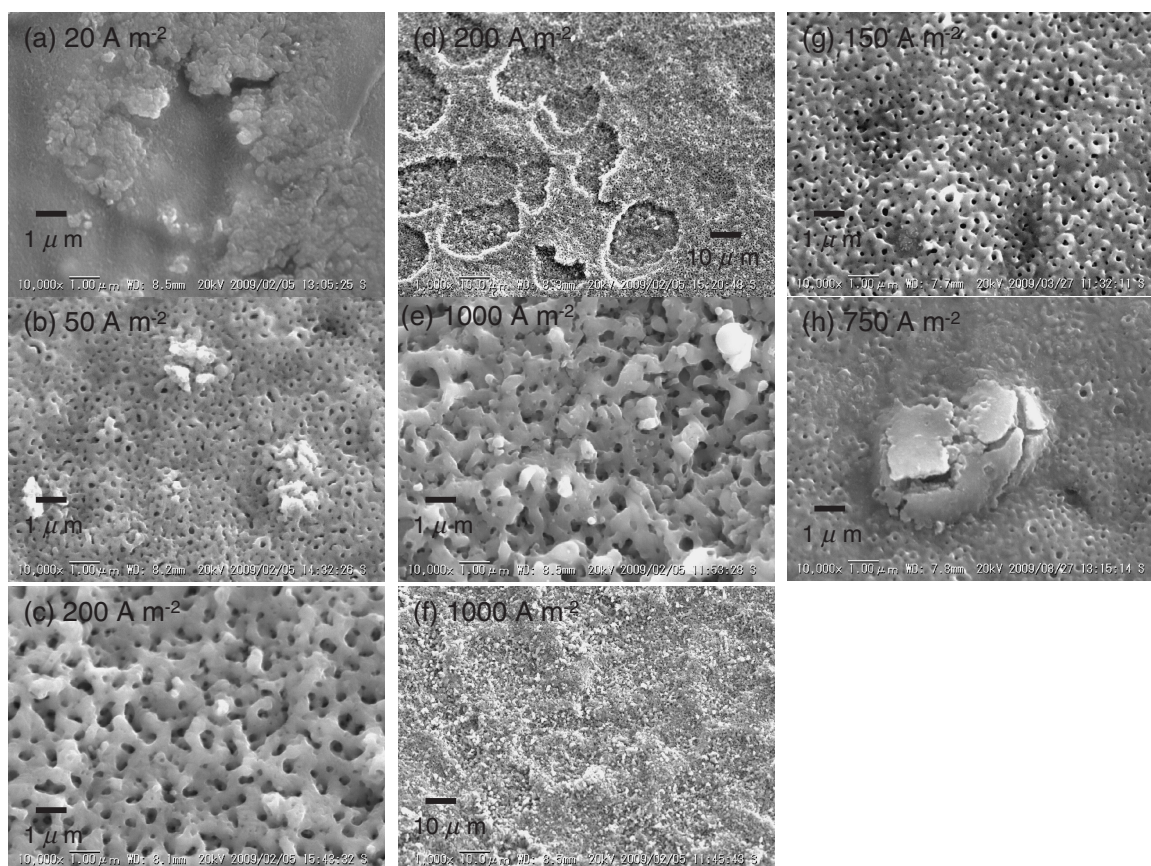


Fig. 1 Surface microstructures of anodized TiO_2 . (a)–(f) and (g)–(h) anodized in 1.2 and 0.1 mol·L⁻¹ sulfuric acid, respectively.

Hinshelwood kinetics model.¹⁵⁾ When the concentration is low, the degradation rate of MB, r , can be simplified to the following apparent first-order equation:

$$r = \frac{dC}{dt} = kKC = k_{\text{app}}C \quad (1)$$

where C is the concentration of MB, t is the duration of light illumination, k is the reaction rate constant, K is the adsorption coefficient of the reactant and k_{app} is the apparent rate constants for MB degradation. In this study, photocatalytic activity is expressed as k_{app} obtained from the slope of t vs $-\ln(C/C_0)$ plots.

3. Results and Discussion

In the process of anodic oxidation, the current rose to the programmed value abruptly (typically within about 1 s) regardless of the anodizing conditions. On the other hand, the applied voltage depended upon the conditions of anodization. High voltage and high sweep rate were attained when the current density was high or the sulfuric acid concentration was low. For example, when titanium was anodized in 1.2 mol·L⁻¹ sulfuric acid with the current of 500 A·m⁻², the initial sweep rate and the final voltage were 6.7 V s⁻¹ and 198.7 V, respectively, which were similar to those previously reported.¹⁶⁾

SEM images of the anodized TiO_2 are displayed in Fig. 1. In the cases of the anodic oxides prepared in an electrolyte of 1.2 mol·L⁻¹ sulfuric acid, nano-sized pores emerged above

the current density of 50 A·m⁻² (Fig. 1(b)) and became larger with the current densities. These nano-sized pores were not observed in the oxide anodize with current density lower than 20 A·m⁻² (Fig. 1(a)). For the anodic oxides prepared with the current density larger than 200 A·m⁻², concave curvature with dozens of micrometers in diameter were confirmed, suggesting spalling of the formed oxide from the surface during the anodization (Fig. 1(d)). When the current density increased up to 1000 A·m⁻², the above concave curvature was not confirmed (Fig. 1(f)). For the anodic oxides prepared in an electrolyte of 0.1 mol·L⁻¹ sulfuric acid, micro-pores were distributed homogeneously in the oxide anodized with current density higher than 150 A·m⁻² (Fig. 1(g)). The sizes and frequencies of the pores did not change in accordance with the current density. Hillocks with several micrometers were observed on the surface anodized with current density higher than 750 A·m⁻² (Fig. 1(h)). However, the concave curvature was not observed regardless of the applied current density.

The crystal structures of the fabricated TiO_2 were investigated by thin layer XRD technique. XRD patterns are shown in Fig. 2(a) and (b). In both cases, when the current density increased, the peak intensity of titanium substrate declined and the peaks from titanium oxides increased. This indicates that thick oxide layer was formed with the increment of the current density. The growth of the oxide layer was also observed in the potentiostatic anodization of titanium with the increment of the applied voltage.¹⁷⁾ In the cases of the anodic oxides prepared in an electrolyte of

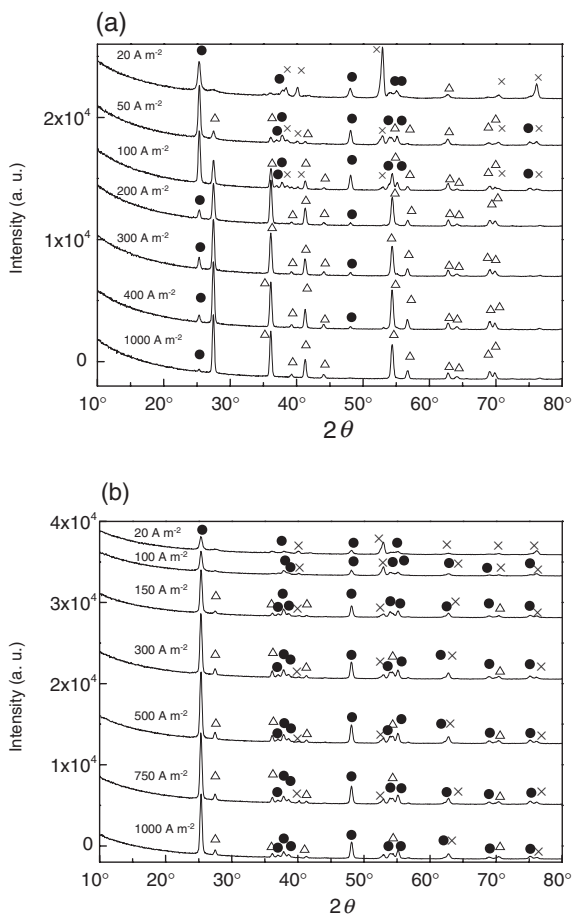


Fig. 2 XRD patterns of TiO_2 anodized with various current density in a sulfuric acid of (a) $1.2 \text{ mol}\cdot\text{L}^{-1}$ and (b) $0.1 \text{ mol}\cdot\text{L}^{-1}$. ●: anatase, △: rutile, ×: titanium.

$1.2 \text{ mol}\cdot\text{L}^{-1}$, anatase phase was confirmed in the oxide and the peak intensity increased with the current density up to $100 \text{ A}\cdot\text{m}^{-2}$. With further increase of the current density, the primary phase changed from anatase to rutile. In the cases of TiO_2 anodized in $0.1 \text{ mol}\cdot\text{L}^{-1}$, the peak intensity of anatase increased with increasing of the current density until $300 \text{ A}\cdot\text{m}^{-2}$ followed by saturation of the intensity. The weak diffraction peaks due to rutile phase were observed irrespective of the current density.

The rutile phase fraction, sizes of the crystallite, and lattice strain of the anodized TiO_2 were calculated. Several empirical equations were proposed to estimate the fraction of the TiO_2 constituent phase between rutile and anatase,^{18–20)} while no distinct difference was found between them. Using eq. (2),²⁰⁾

$$f_{\text{rutile}} = \frac{0.679 \cdot I_{\text{rutile}}}{I_{\text{rutile}} + I_{\text{anatase}}} + 0.312 \left(\frac{I_{\text{rutile}}}{I_{\text{rutile}} + I_{\text{anatase}}} \right)^2 \quad (2)$$

where $I_{\text{anatase}101}$ and $I_{\text{rutile}110}$ are the peak area of the main anatase and rutile reflections, respectively, the fractions of rutile in the anodic oxides were calculated. Hall's equation (eq. (3)) was employed to calculate the sizes of crystallite and lattice strain,²¹⁾

$$\beta \cdot \cos \theta = K \cdot \frac{\lambda}{L} + 2\varepsilon \cdot \sin \theta \quad (3)$$

where L is crystallite size expressed in nm, λ is the X-ray wavelength, β is the full width at half maximum (FWHM) of the signal in radians, K is the shape factor of 0.89, assuming that the crystallite is sphere, ε is lattice strain, and θ is the Bragg angle. The intensity and the FWHM were obtained by software of Profile Fit (Philips, Netherlands). For the oxide anodized with the low current density ($20 \text{ A}\cdot\text{m}^{-2}$ for $1.2 \text{ mol}\cdot\text{L}^{-1}$ and lower than $100 \text{ A}\cdot\text{m}^{-2}$ for $0.1 \text{ mol}\cdot\text{L}^{-1}$ sulfuric acid), the plotted data could not fit with Hall's equation due to low intensity of the diffraction peaks. Thereby, the lattice strain and crystallite size of the predominant phase were calculated for the oxides with higher current density. The result is shown in Fig. 3. The fraction of rutile (Fig. 3(a)) was 58% and above 90% in the anodic oxide with the current density of $150 \text{ A}\cdot\text{m}^{-2}$ and $500 \text{ A}\cdot\text{m}^{-2}$, respectively, when the concentration of sulfuric acid in the electrolyte was $1.2 \text{ mol}\cdot\text{L}^{-1}$. In the cases of the anodic oxides prepared in an electrolyte of $0.1 \text{ mol}\cdot\text{L}^{-1}$, the rutile fraction was less than 10% regardless of the current density. With increasing of the current density, the size of the crystallite and the lattice strain decreased and converged to 30–40 nm and $2\text{--}3 \times 10^{-3}$, respectively (Fig. 3(b) and (c)).

Figure 4(a) shows the rate constants for MB degradation of the anodic oxides prepared in an electrolyte of $1.2 \text{ mol}\cdot\text{L}^{-1}$, revealing the rate constants increased with the current density and reached the plateau at the current density above $200 \text{ A}\cdot\text{m}^{-2}$. On the other hand, TiO_2 anodized in an electrolyte of $0.1 \text{ mol}\cdot\text{L}^{-1}$ sulfuric acid degraded MB with almost same low rate constants independent of the current density. The surface area increased with the current density shown in Fig. 4(b). It should be noted that the effective surface area derived in this study is corresponding to the illuminated area to evaluate photocatalytic activity, because photocatalytic reaction occurs at the illuminated area. This implies that the surface area derived from BET method is inadequate to consider the photocatalytic activities, because it provides the surface area including the area not to be illuminated. Specific surface area of the anodic oxides prepared in an electrolyte of $1.2 \text{ mol}\cdot\text{L}^{-1}$ sulfuric acid linearly increases with the current density and reached plateau at $500 \text{ A}\cdot\text{m}^{-2}$, whereas the surface area was quite low regardless of the current density for the anodized TiO_2 prepared in an electrolyte of $0.1 \text{ mol}\cdot\text{L}^{-1}$. From these results, it was found that the surface morphologies including roughness depended on the concentration of sulfuric acid in the electrolyte preferentially as compared with the current density and the final voltage.

It was reported that the photocatalytic activities were affected by different factors such as crystallinity, crystal structure, surface area, chemical impurities, and constituent phase and its fraction. TiO_2 photocatalyst is one of the heterogeneous catalysts, so that the activities are improved by absorbing large amount of substances to be photo-degraded on the surface of TiO_2 with high surface area. In the present study, the anodized TiO_2 with higher surface area exhibited higher activity. In order to investigate the photocatalytic activities per surface area of TiO_2 , specific rate constant (SRC) was defined. The SRC dependence upon the current density was shown in Fig. 4(c). It reveals that TiO_2 anodized in an electrolyte of $1.2 \text{ mol}\cdot\text{L}^{-1}$ sulfuric acid showed better performance as compared with that of

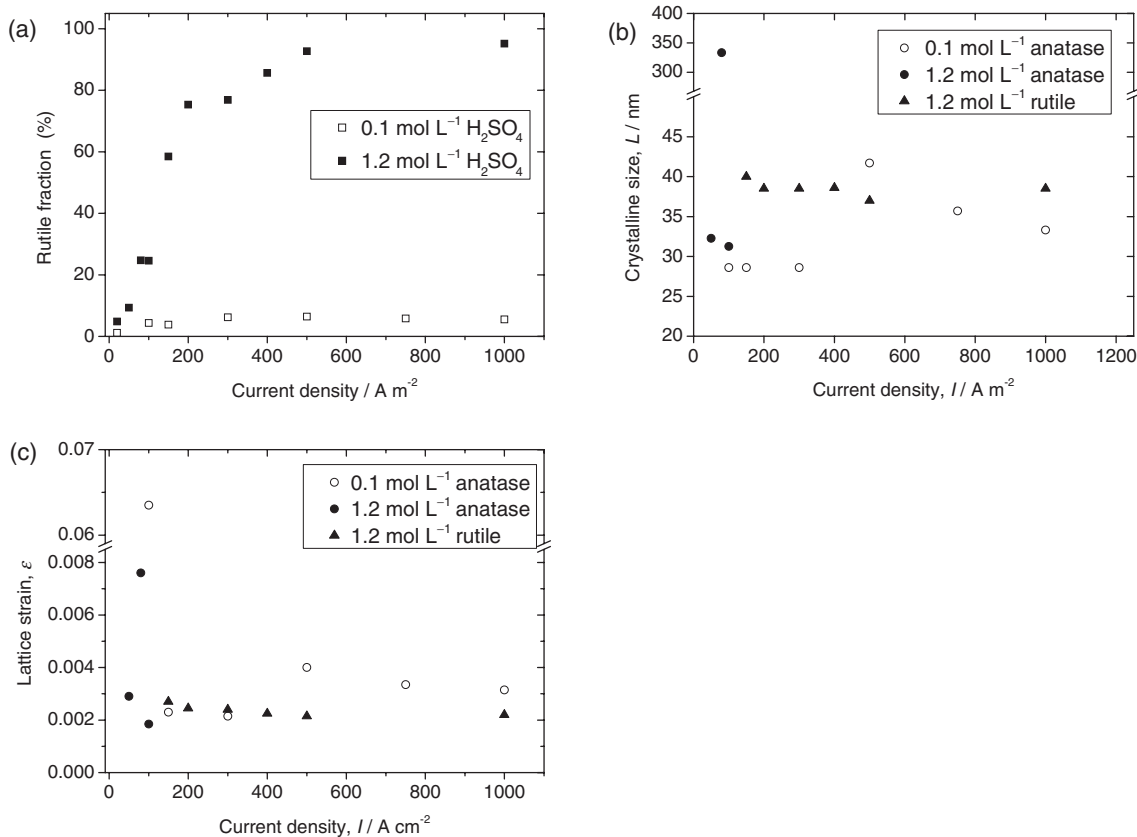


Fig. 3 Dependence of (a) rutile phase fraction in the oxide, (b) crystallite size, and (c) lattice strain of the oxide upon the current density.

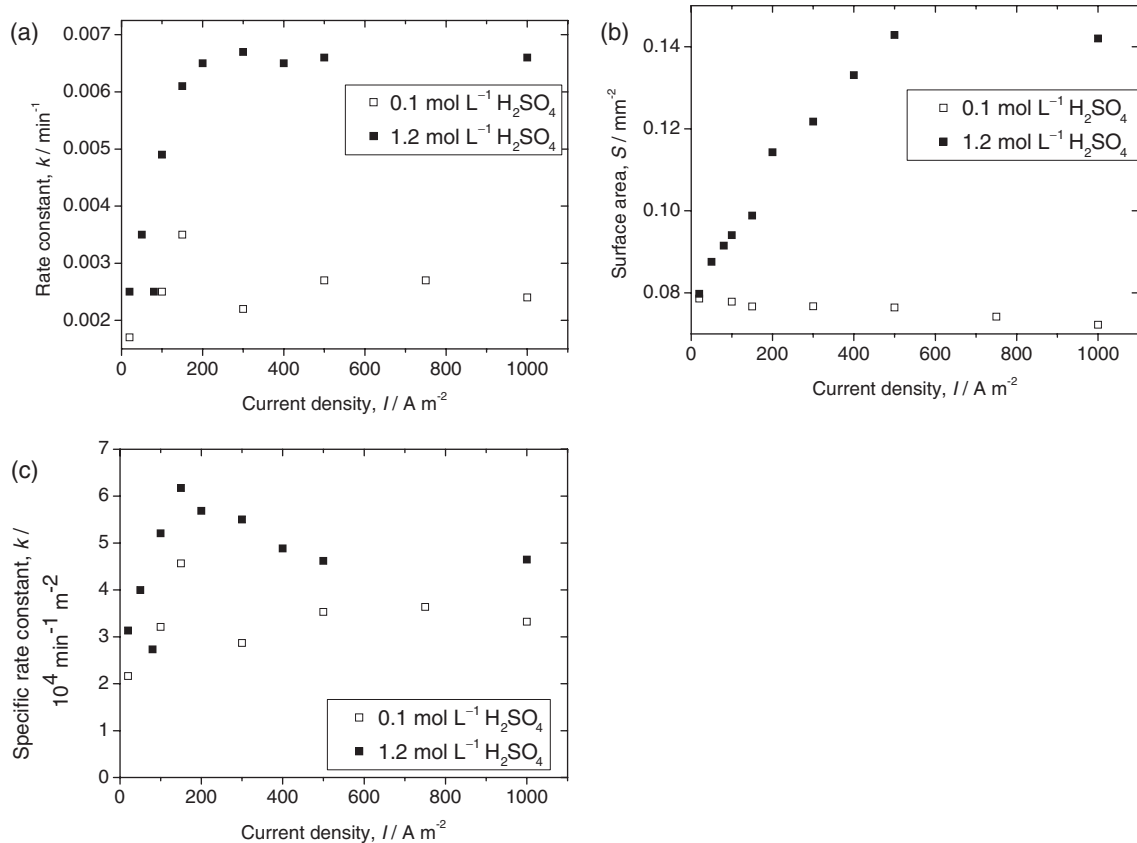


Fig. 4 (a) MB degradation rate constants, (b) surface area of anodized TiO₂ and (c) specific rate constants for photocatalytic MB degradation.

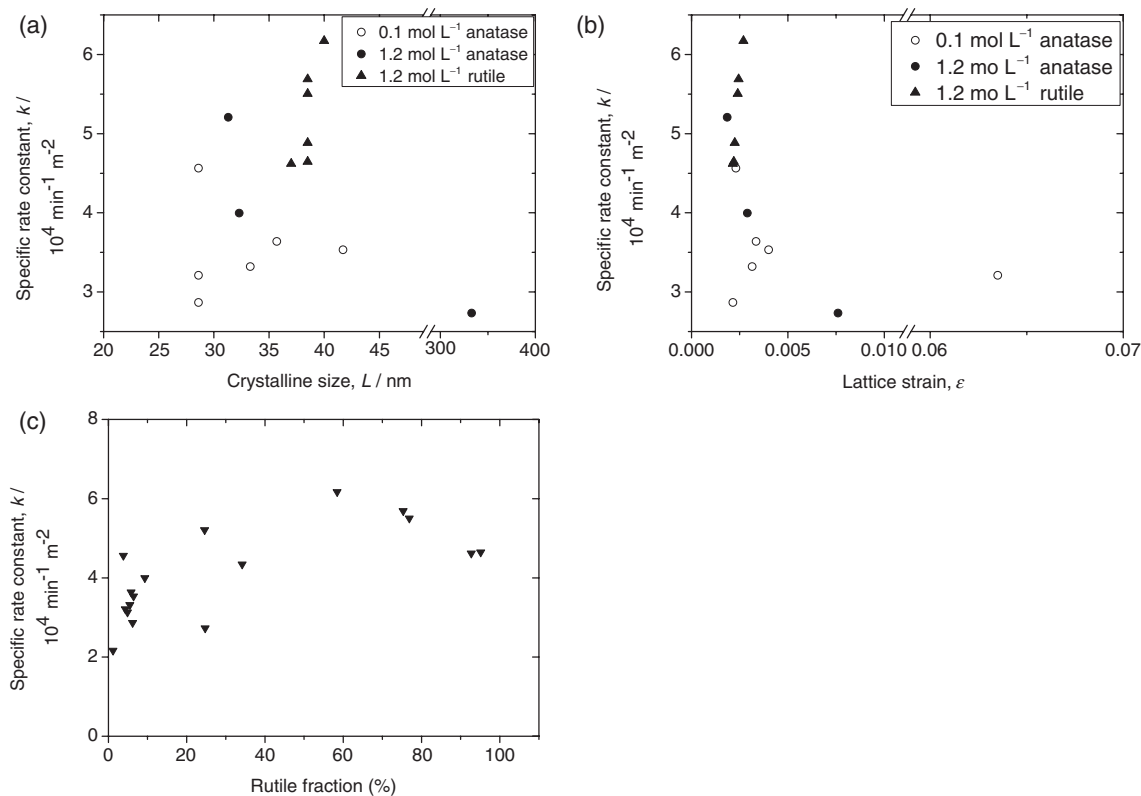


Fig. 5 Dependence of specific rate constant for MB degradation upon (a) crystallite size, (b) lattice strain and (c) rutile fraction.

0.1 mol·L⁻¹ and reached the peak with the current density at 150 A·m⁻².

The SRC dependences on crystallite size, lattice strain and phase composition (rutile fraction) are summarized in Fig. 5. The plotted data is relatively scattered due to low intensity in reflection, especially for the anodic oxides prepared in the electrolyte of low sulfuric acid concentration. However, it is possible to consider the correlation between the crystallographic factors and SRC to a certain extent, because reasonable explanation to understand this result could be provided as stated below. With the increment of the crystallite size, the SRC increased and showed the highest at 40 nm in the crystallite size as shown in Fig. 5(a). If the crystallite is small, it is considered that the photocatalytic activity is deteriorated because a lot of interfaces could become sink sites for the photo-excited charge carriers of electrons and holes.^{22,23} In addition, since electrons and holes can not migrate a longer distance in the small crystallite and they can not effectively separate, the recombination of the charge carriers may occur more frequently in smaller crystalline than in larger one.²⁴ On the other hand, the adsorbed amounts of molecules to be decomposed on the surface of the photocatalyst decrease with increasing crystallite size.²⁵ Further, the photo-excited charge carriers can not reach the surface of the photocatalyst due to an increase of recombination frequency, resultantly the photo-degrade efficiency is lowered. It is plausible that there exists an optimum crystallite size due to this opposite two factors as shown in Fig. 5(a). The optimum crystallite size of 40 nm in the current study is interestingly in the range of the reported crystallite size.²⁶

The anodized TiO₂ showed high activities with low lattice strain as shown in Fig. 5(b). The crystal strain is reported to scatter the charge carriers and interrupt their migrations to the catalysts surface,^{27–29} which could provide reasonable explanation to the present result.

The SRC increased with an increase of rutile fraction (Fig. 5(c)). The highest activity marked in the oxide with about 60% rutile phase, which is higher than 25% of commercially available photocatalyst P-25.³⁰ It is generally accepted that high photoactivity could be obtained in the TiO₂ of anatase single phase or a mixed phase of a large amount of anatase and residual rutile. Slightly higher Fermi level of anatase to rutile phase³¹ could be attributable to the higher performance of anatase. However, there are different studies to report the similar photocatalytic activities between them³² or superiority of rutile to anatase.^{33,34} This disagreement is originated from the various parameters which can not be simultaneously controlled, such as specific surface area, distribution of pore size and crystallinity. In contrast, the present method enables us to control the crystallite size, lattice strain, phase component by changing current density. The rutile structured TiO₂ anodized in 1.2 mol·L⁻¹ sulfuric acid aqueous solution with the current density of 1000 A·m⁻² (rutile fraction: 95.2%, crystallite size: 38.5 nm, lattice strain: 0.0022) exhibited higher SRC than anatase structured TiO₂ anodized in 0.1 mol·L⁻¹ sulfuric acid aqueous solution with the current density of 1000 A·m⁻² (rutile fraction: 5.5%, crystallite size: 38.5 nm, lattice strain: 0.00315). These results suggest that the rutile structured TiO₂ with superior photocatalytic activities could be fabricated by controlling electrochemical parameter in the anodic oxidation.

4. Conclusions

The characteristics, including phase composition and crystallinity, of the TiO₂ fabricated by anodic oxidation were systematically examined by controlling the current density. The anodic oxide with low lattice strain and the crystallite size of appropriately 40 nm showed high SRC for MB degradation. It was also elucidated that TiO₂ consisting of rutile phase with high crystallinity exhibited superior photocatalytic activity to anatase phase.

Acknowledgements

The authors wish to thank Ms. Y. Matsuda and Mr. S. Sugiyama from IMR, Tohoku University, for their helpful assistance. The authors are grateful to Keyence Co., Ltd. for the measurements of surface areas by a laser microscopy.

REFERENCES

- 1) A. Fujishima and K. Honda: *Nature* **238** (1972) 37–38.
- 2) N. Negishi, T. Iyoda, K. Hashimoto and A. Fujishima: *Chem. Lett.* **24** (1995) 841–842.
- 3) U. Backman, A. Auvinen and J. K. Jokiniemi: *Surf. Coat. Technol.* **192** (2005) 81–87.
- 4) T. P. Curtis, G. Walker, B. M. Dowling and P. A. Christensen: *Water Res.* **36** (2002) 2410–2413.
- 5) D. Dumitriu, A. R. Bally, C. Ballif, P. Hones, P. E. Schmid, R. Sanjinés, F. Lévy and V. I. Pârvulescu: *Appl. Catal. B* **25** (2000) 83–92.
- 6) K. Shankar, K. C. Tep, G. K. Mor and C. A. Grimes: *J. Phys. D: Appl. Phys.* **39** (2006) 2361–2366.
- 7) D. Velten, V. Biehl, F. Aubertin, B. Valeske, W. Possart and J. J. Breme: *Biomed. Res.* **59** (2002) 18–28.
- 8) A. G. Mantzila and M. I. Prodromidis: *Electrochim. Acta* **51** (2006) 3537–3542.
- 9) T. Shibata and Y.-C. Zhu: *Corros. Sci.* **37** (1995) 253–270.
- 10) R. Palombari, M. Ranchella, C. Rol and G. V. Sebastiani: *Sol. Energy Mater. Sol. Cells* **71** (2002) 359–368.
- 11) N. Masahashi, Y. Mizukoshi, S. Semboshi and N. Ohtsu: *Applied. Catal. B* **90** (2009) 255–261.
- 12) N. Masahashi, Y. Mizukoshi, S. Semboshi and N. Ohtsu: *Chem. Lett.* **37** (2008) 1126–1127.
- 13) Y. Mizukoshi, N. Ohtsu, S. Semboshi and N. Masahashi: *Appl. Catal. B* **91** (2009) 152–156.
- 14) S. Ahn, L.-K. Choi and J. Jung: *J. Adv. Oxid. Technol.* **10** (2007) 354–360.
- 15) I. K. Konstantinou and T. A. Albanis: *Appl. Catal. B* **49** (2004) 1–14.
- 16) M. V. Diamanti and M. P. Pedferri: *Corros. Sci.* **49** (2007) 939–948.
- 17) N. Masahashi, S. Semboshi, N. Ohtsu and M. Oku: *Thin Solid Films* **516** (2008) 7488–7496.
- 18) D. Chen, D. Yang, Q. Wang and Z. Jiang: *Ind. Eng. Chem. Res.* **45** (2006) 4110–4116.
- 19) R. A. Spurr and H. Myers: *Anal. Chem.* **29** (1957) 760–762.
- 20) X. Fu, L. A. Clark, Q. Yang and M. A. Anderson: *Environ. Sci. Technol.* **30** (1996) 647–653.
- 21) G. K. Williamson and W. H. Hall: *Acta Metall.* **1** (1953) 22–31.
- 22) H. Kominami, J. Kato, M. Kohno, Y. Kera and B. Ohtani: *Chem. Lett.* **12** (1996) 1051–1052.
- 23) F. Amano, O.-O. Preto-Mahaney, Y. Terada, T. Yasumoto, T. Shibayama and B. Ohtani: *Chem. Mater.* **21** (2009) 2601–2603.
- 24) K. Tanaka, M. F. V. Capule and T. Hisanaga: *Chem. Phys. Lett.* **187** (1991) 73–76.
- 25) O. Carp, C. L. Huisman and A. Reller: *Prog. Solid State Chem.* **32** (2004) 33–177.
- 26) M. Inagaki, R. Nonaka, B. Tryba and A. W. Morawski: *Chemosphere* **64** (2006) 437–445.
- 27) A. G. Agrios and P. Pichat: *J. Photochem. Photobiol. A* **180** (2006) 130–135.
- 28) G. Benkő, B. Skårman, R. Wallenberg, A. Hagfeldt, V. Sundström and A. P. Yutsev: *J. Phys. Chem. B* **107** (2003) 1370–1375.
- 29) J. Wu, X. Lu, L. Zhang, F. Huang and F. Xu: *Eur. J. Inorg. Chem.* **2009** (2009) 2789–2795.
- 30) T. Ohno, K. Sarukawa, K. Tokieda and M. Matsumura: *J. Catal.* **203** (2001) 82–86.
- 31) H. P. Maruska and A. K. Ghosh: *Solar Energy* **20** (1978) 443–458.
- 32) X. Deng, Y. Yue and Z. Gao: *Appl. Catal. B: Environ.* **39** (2002) 135–147.
- 33) A. Mills, S. K. Lee and A. Lepre: *J. Photochem. Photobiol. A: Chem.* **155** (2003) 199–205.
- 34) S. S. Watson, D. Beydoun, J. A. Scott and R. Amal: *Chem. Eng. J.* **95** (2003) 213–220.